Study on the optimal layout of helioscope field based on genetic algorithm

Ziyue Song[1,*], Tingyu Yang[1], Siqi Li[2]

[1]Department of Economic Statistics, Henan University, Henan, China, 475004

[2]Departmentof Financial Mathematics, Henan University, Henan, China, 475004

* Corresponding Author Email: Songzy0322@163.com

Abstract. The tower photovoltaic power plant particularly depends on the proper arrangement of the heliostat field, which is a crucial component of the tower solar power system and costs between 40% and 50% of the tower solar power plant's overall investment expenses. In this study, an optimization model is established under the restrictions of the heliostat mirror's size and placement parameters. Then, using numerical optimisation tools such as the simulated annealing algorithm and genetic algorithm, the layout of the heliostat field is repeatedly calculated in order to determine the ideal configuration for the heliostat field, which will maximize its yearly thermal power output. This paper has some significance in optimizing the layout of the heliostatic field.

Keywords: Heliostat field, Genetic algorithm, Simulated annealing method.

1. Introduction

A new clean energy technology that is low-carbon and environmentally favorable is solar energy[0]. A suitable configuration of the helioscope field is especially crucial for the tower solar thermal power station because the heliostat field, a crucial component of the concentrating system, accounts for roughly 40%–50% of the power plant's total investment costs[2]. It also directly impacts the heat absorption tower's energy absorption scale[3]. Optimizing the mirror field has emerged as a critical component in the design process to increase the power plant's overall cost performance[4].

Numerous academics both domestically and internationally have researched the mirror electric field's optimization design. Rizvi Arslan A and Yang Dong focuses on the famous center point projection method and its implementation[5].In Seonghyeok Yang, Kyungeun Lee and Ikjin Lee's paper,the alternating direction method is proposed to perform heliostat field layout optimization[6]. Wang Wen-Qi, Jiang Rui, He Ya-Ling and Li Dong present three gradually sparse biomimetic (GSB) heliostat field layouts, which gradually extend from the inside to the outside[7].While the position state of the heliostat can be studied by these investigations, the majority of them overlook the collector's shadow and the solar light's distinct treatment.

This paper adopts a genetic algorithm and simulated annealing method to study on the optimal layout of helioscope field[8]. The design of the heliostat field is helpful to promote the development of tower solar thermal power generation.

2. Problem description and model building

2.1. Question description

Tower power stations are primarily made up of a heliostat and collector. The heliostat's key operating principle is that sunlight reflection placed in the field on top of the collector heats the heat conduction medium and stores solar energy as heat energy, which is subsequently converted to electricity through heat exchange. The heliostat's base is made up of a horizontal axis and a longitudinal shaft, with the horizontal axis situated on a plane mirror. The mirror's pitch angle can be adjusted by the horizontal axis, and its azimuth angle can be adjusted by the longitudinal axis. The heliostat's normal direction varies in tandem with changes in the sun's position, allowing the tapering solar light reflected by the heliostat's center to point in the direction of the collector's center. The

heliostat is lined with many heliostats and has an absorption tower with a collector at the top. The collector stores the heat produced by the absorbed solar radiation and then turns it into electricity.

It is known that all helioscopes have the same size and installation height when the rated average yearly output thermal power of the heliostat field is 60 MW. Design factors include the absorption tower's position coordinates, the size, quantity, placement, and height of the heliostat. Ensure that these parameters are designed to maximize the average yearly average output thermal power per unit mirror area.

2.2. Model establishment

The absorber's position, the heliostat's size, and the initial number are fixed when the parameters are first initialized. Next, based on a specified parameter configuration, the fitness function is created to determine the annual average output thermal power per unit mirror area. The ideal configuration and optimal solution for the unknown parameters are then found via simulated annealing. Using the same procedure, the next variable is found as the fixed value of this argument. The best option for each parameter is the one that maximizes the yearly average output thermal power per unit of mirror area. Ultimately, an assessment was conducted to confirm that the generated configurations meet every conditional criterion.

Suppose that the heliostat field adopts the EB layout[9] which is shown in Figure 1.

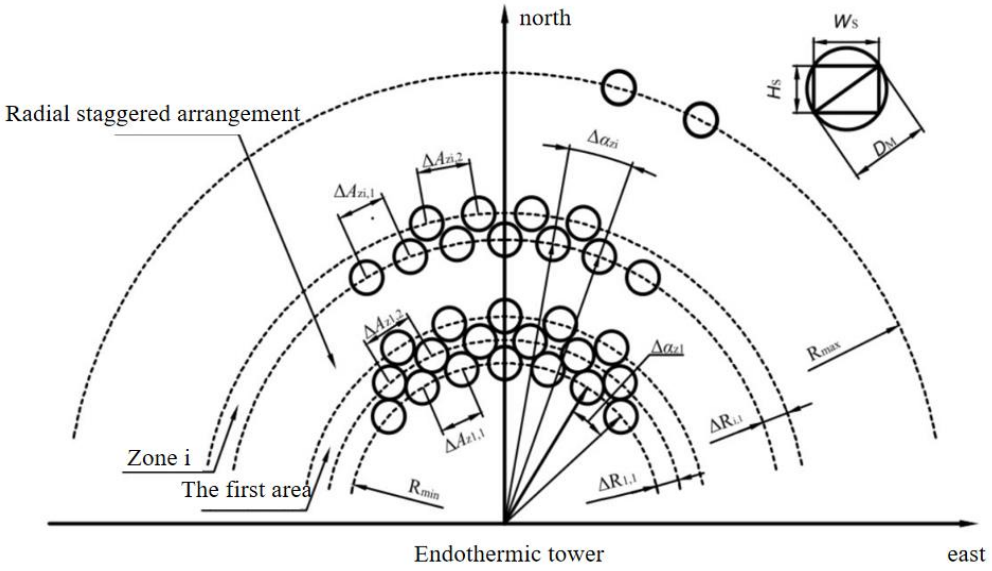


Figure 1. EB layout diagram

The calculation formula of the first ring in each area of the mirror field is as follows, where A_{sf} is the azimuth spacing factor and its value is mainly related to the tower height, usually the value is 2.

$$\Delta A_{Z,i} = \Delta A_{z2,2} = A_{sf} \times W_S . \tag{1}$$

Except for the first ring in each region,other heliostine azimuth spacing calculation formula is as follows, where $\Delta A_{zi.j}$ is the azimuth spacing of the j-ring heliostat in the i-region of the mirror field.

$$\Delta A_{zi.j} = 2R_{i.j} * \sin(\Delta\alpha_{Z.i} / 2) , \tag{2}$$

$$\Delta\alpha_{Z.i} = 2arc\sin[\Delta A_{z,1} / (2R_{i.1})] . \tag{3}$$

The radial spacingat the junction of adjacent mirror fields is constant set to ΔR=DM[10].

The formula for calculating the radial spacing between the first ring and the second ring in the first region of the mirror field:

$$\Delta R_{i.1} = \sqrt{D_M^2 - (\Delta A_{z,1} / 2)^2} \,. \tag{4}$$

Conical light discretization treatment: The reflected light of the tapered sun is transformed into several rays through radial and circular directions, and each light contains equal solar radiation energy, which is *E*.

The discretization diagram of cone light is shown in Figure 2.

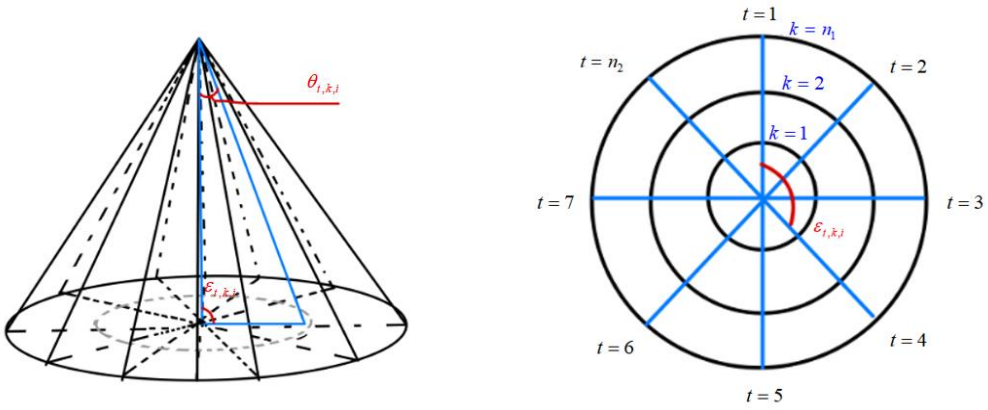


Figure 2. Disdispersion of tapered light

First, make n_1 tacone light bottom diameter into a number of parts, the length of each part $\Delta r = \frac{r}{n_1}$. Second, make the circumference of the conical light n_2, the center corner of each part $\Delta\varepsilon = \frac{360^\circ}{n_2}$. Thus, the cone light is discretized into a $n_1 \times n_2$ strips of light.

For the cone reflected light at a point on the i-face heliostat, the cone angle of the beam formed by the radial *k* th portion $\left(k \in [1, n_1]\right)$ and the circumferential *t* th is (see the top angle in the shaded region). $\left(t \in [1, n_2]\right)$.

The calculation method is provided as follows, where 2λ is the maximum conical angle of a conical light; λ is a constant related to sunlight.

$$\theta_{t,k,i} = \frac{\lambda}{n_1} k, k = 1, 2, ..., n_2 \,. \tag{5}$$

The azimuth of the bottom radius of the light cone whose height is a unit of length is $\varepsilon_{t,k,i}$ (the circumference of the ground).

$$\varepsilon_{t,k,i} = \frac{360^\circ}{n_2}(t-1), t = 1, 2, ..., n_1 \,. \tag{6}$$

After the discretization, any one discrete light vector can be obtained. $\vec{d}_{t,k,i}$ is an arbitrary vector on the bottom surface of the conical light line.

$$\vec{e}_{t,k,i} = \vec{R}_i + \vec{d}_{t,k,i} \,. \tag{7}$$

Establish a function for the position of the absorption tower, coordinate, heliostat size, installation height, number of heliostats, and position of heliostat.

$$f(w_1) = (x_1, y_1, z_1, m, n, h+n, N, x_m, y_m, z_m) \,. \tag{8}$$

The objective function is the output thermal power of the helioscope field:

$$S = E_{field} = DNI * \sum_{i}^{N} A_i \vartheta_i , \tag{9}$$

where *DNI* is the normal direct radiation irradiance; *N* is the total number of heliostat.

Step1 Take a condition as the initialised solution of *f(w0)*. For example, when $(x_1, y_1, z_1) = (0,0,80)$; $m = 6$, $n = 6$; $h + n = 4$; $N = 1746$,

$$f(w_0) = (0,0,80,6,6,4,1746, x_m, y_m, z_m), \tag{10}$$

where (x_m, y_m, z_m) is the coordinate of the heliostat position.

The average annual output thermal power at this time is E^o_{field}.

$$S = E^0_{field} = DNI * \sum_{i}^{N} A_i \vartheta_i . \tag{11}$$

Step2 Using *h* as a variable with a step length of 1 m, produce a new solution $f(w_n)$.

$$f(w_n) = (x_1, y_1, z_1, m, n, h + n, N, x_m, y_m, z_m). \tag{12}$$

For example, when *i*=1, $f(w_1) = (0,0,81,6,6,4,1746, x_m, y_m, z_m)$.

Step3 Calculate the objective function difference corresponding to the new solution.

$$\Delta t = S - S'. \tag{13}$$

If $\Delta t < 0$ the new solution *S'*is accepted as the new current solution . Otherwise, accept the new solution *S'* as the new current solution *S* with probability $e^{-\Delta t/T}$.

Step4 Upon acceptance, the new solution replaces the current one,only implementing the portion of the current solution that corresponds to the new solution for transformation purposes and correcting the value of the target function. The existing solution only carries out one iteration at this time. To begin the subsequent testing cycle based on this. The trial's subsequent phase is predicated on the initial existing solution in the event that the new solution is deemed to be abandoned. When the new solution is judged to be abandoned, the next round of the trial is based on the original current solution.

In conclusion, obtain the following mathematical model:

The constraint conditions are as follow:

1. Heliostat size constraint: The width of heliostat w_s is not less than the mirror height H_s.

$$W_S \geq H_S . \tag{14}$$

2. Mirror width and mirror height constraint: Heliostat side length must be between 2 m and 8 m.

$$\begin{cases} 2 \leq W_S \leq 8 \\ 2 \leq H_S \leq 8 \end{cases}. \tag{15}$$

3. Installation height constraint: The installation height of the heliostat must be between 2 m and 6 m.

$$2 \leq h_i \leq 6 . \tag{16}$$

4. Tower construction position constraint: The absorber must be located in the circular heliostat field region. Therefore, the distance between the absorption tower and the center of the heliostat field L_1 must be less than the radius of the circular heliostat field.

$$0 \leq L_i \leq 350 . \tag{17}$$

5. Adjacent heliostat position constraint: The distance between the centers of the adjacent heliostat

base is at least 5 m longer than the mirror width.

$$L_{i,\ j} - W_S \geq 5, i = 1, 2, ..., N,\ j = 1, 2, ..., N, i \neq j\ . \tag{18}$$

where $L_{i,j}$ is the distance between the center of the i-face helioscope and the base of the j-face helioscope.

6. Hyiostat position constraint: The heliostat must be within the helstat field and the distance from the absorber must exceed 100 m.

$$\begin{cases} X_i^2 + Y_i^2 \leq 350^2 \\ X_i^2 + \left(Y_i + L_i\right)^2 \geq 100^2 \end{cases}. \tag{19}$$

In the mirror field coordinate system *XYZ*, the coordinates of the i-face heliostat are $p_i\left(x_i, y_i, z_i\right)$; the coordinates of the absorber are $I\left(0, L_1, H_t\right)$.

7. Heliostat field rated power constraint: The heliostatic field must reach a rated power of 60 MW.

$$\frac{1}{60}\sum_{D=1}^{60}(DNI\sum_{i=1}^{N}A_i\eta_i) \geq 60MW\ . \tag{20}$$

8. Height constraint of the heliostat field mirror: The installation height needs to be greater than the mirror height below the horizontal.

$$\frac{H_S}{2} \leq h_i\ . \tag{21}$$

The optimized model:

$$\max \frac{\frac{1}{60}\sum_{D=1}^{60}(DNI\sum_{i=1}^{N}A_i\eta_i)}{\sum_{i=1}^{N}A_i}, \tag{22}$$

$$s.t.\begin{cases} W_S \geq H_S \\ 2 \leq W_S \leq 8 \\ 2 \leq H_S \leq 8 \\ 2 \leq h_i \leq 6 \\ 0 \leq L_i \leq 350 \\ L_{i,j} - W_S \geq 5, i = 1, 2, \cdots, n,\ j = 1, 2, \cdots, n, i \neq j\ . \\ X_i^2 + Y_i^2 \leq 350,\ X_i^2 + \left(Y_i + L_i\right)^2 \geq 100^2 \\ \frac{1}{60}\sum_{D=1}^{60}\left(DNI_D\sum_{i=1}^{n}A_i\eta_i\right) \geq 60MW \\ \frac{H_S}{2} \leq h_i \end{cases} \tag{23}$$

3. Results and discussion

Through calculation, the average optical efficiency and output power of the heliostatic field on the 21st per month are shown in the Figure 3:

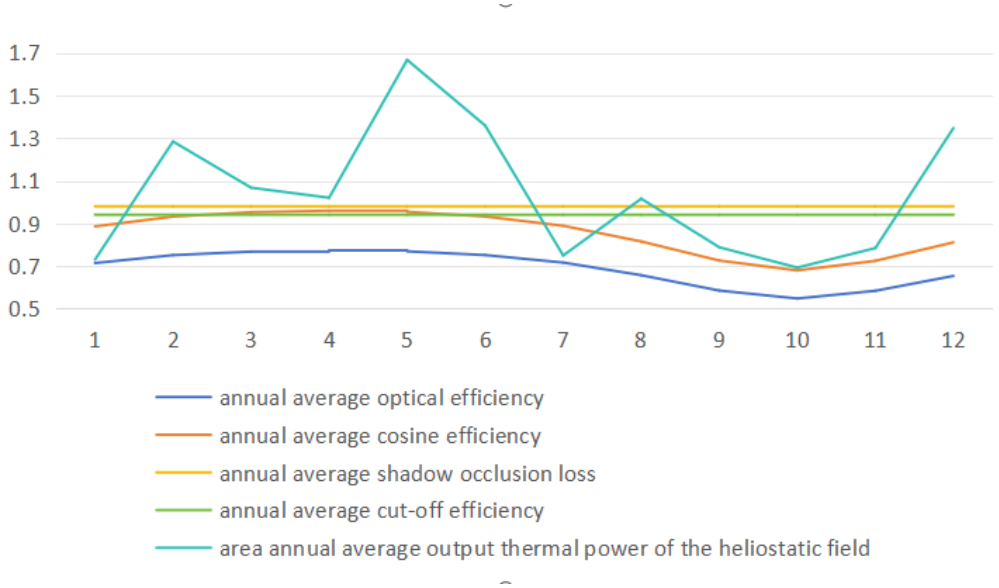


Figure 3. Average optical efficiency and output power on 21st per month

The annual average optical efficiency and output power of the heliostatic field can be calculated as shown in Table 1:

Table 1. Average optical efficiency and output power

annual mean optical efficiency	Annual average cosine efficiency (physics)	Annual average shadow occlusion efficiency	Annual mean Cut off efficiency	Annual average output thermal power (MW)	Annual output thermal power per unit area (kW/m^2)
0.688937	0.854881	0.98	0.940444	62.179504487237	1.208542361

Table 1 shows the annual average optical efficiency, annual average cosine efficiency, annual average shadow occlusion loss, annual average cut-off efficiency, annual average output thermal power and annual average output thermal power per unit area of the heliostatic field, which provides reference for the layout optimization design of the heliostatic field.

Figure 3 displays average optical efficiency and output power on 21st per month. The output thermal power of the heliostat in summer is greater than that in winter. From January to December, the output power of the heliostat firstly increases and then decreases, and the maximum value occurs in June. The reason for this may be that the direct solar radiation radiates in the northern hemisphere to the heliostat more in summer than in winter. The average cosine efficiency and average optical efficiency are seasonal, and the average shading efficiency and average truncation efficiency are less related to the date.

The atmospheric transmittance and mirror do not change with month, which is because the atmospheric transmittance is only related to the distance between the center of the heliostat and the the center of Endothermic tower. When the heliostatic position is determined, the average atmospheric transmittance is calculated to be 0.965, and the mirror reflectivity is determined to be 0.92 according to the assumptions of the model.

The average shade occlusion efficiency is close to 1, which is extremely high. Because of the long distance between the heliostats, the minimal shadow occlusion is low. And the shadow occlusion efficiency is only affected by the shadow occlusion of the heat absorption tower to the heliostat.

The average truncation efficiency is relatively high, reaching about 0.94. Due to the fact that the helophoscope is similar to the vertical section rectangle of the collector, the overflow areas are small, causing small truncation loss.

The average cosine efficiency is relatively low. The highest average cosine efficiency occurs in June, reaching about 0.95, which is because the average cosine efficiency depends on the cosine value of the solar incidence angle. Considering the distance between the heliostat and the heat absorption

tower, the large solar incidence angle and the small cosine value, the average cosine efficiency is relatively small. Average cosine efficiency is symmetrical about June because the sun height angle is symmetrical about June. The average optical efficiency is similar to the average cosine efficiency in distribution, which is because the average cosine efficiency is higher, close to 1. So conclusion can be drawn that only the average cosine efficiency has a significant effect on the average optical efficiency.

After iteration, the optimal layout of the helioscope field is shown in Figure 4:

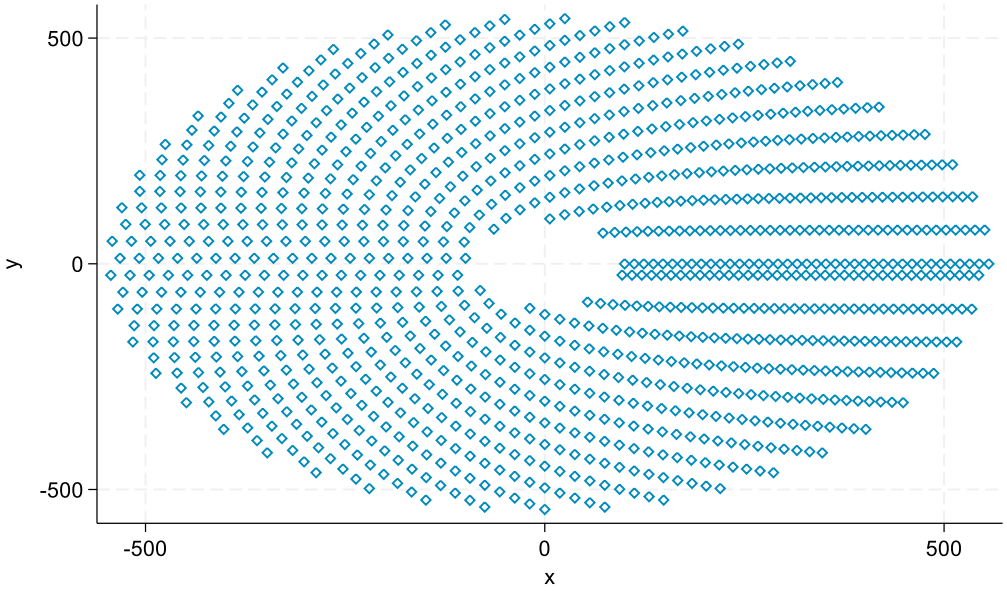


Figure 4. Optimal layout of the helioscope field

Although E^{o}_{field} is related to the optical efficiency and the area of the the panel, the optical efficiency changes little. Therefore, in order to reach the rated power of 60 MW, the width to make sure the area of the heliostat as large as possible is necessary to design. After that,the size, the number and the position of the heliostat can be designed. It can be described as that heliostats are arranged as many as possible in the ring with inner diameter r=100m and outer diameter r=350m. Figure 4 displays optimal layout of the helioscope field. This layout is conducive to better using light and reduce heat loss.

The size parameters of the heliostat field can be designed through genetic algorithm iteration as shown in the Table 2 below:

Table 2. Designing Parameters

absorbing tower's position coordinates	Heliostat's size (Length times width)	Heliostat's installation height(m)	Heliostat's number	Heliostat's total area (m^2)
(0,0)	7×7	4	1050	51450

Under the assumption of EB layout, the optimal layout is obtained by using the numerical optimization algorithm as shown in the Table 1. The absorption tower is located in the center of the heliostat field, and the heliostat is located around the absorption tower as EB layout. The size parameters of the heliostat field are shown in Table 2.

4. Conclusion

The size and location limits of the absorption tower and the heliostats are set in this work assuming that the heliostat field follows the EB layout. This paper firstly establishes the heliostat field's layout parameters by using the optimization model and the optimization algorithm. Once the ideal layout is found, the heliostat field's size parameters are ascertained to maximize its annual thermal power output. The heliostat is positioned using the EB configuration around the absorption tower, which is

positioned in the middle of the heliostat field. The size of the heliostat is designed as 7 m*7 m and the mounting height of the heliostat is designed as 4 m. The total number of heliostats is designed as 1050. This paper provides advance ideas for the optimal layout design of the heliostat field and contributes to lowing the cost of solar power tower system.

References

[1] Yang M. Study on the Optimal Design of Fixed-Sun Mirror Field Based on Variable Step Size Traversal Methods [J]. Academic Journal of Computing Information Science, 2023, 6(12):

[2] N. A Y, Durgesh K, H. V D, et al.Economically feasible solutions in concentrating solar power technology specifically for heliostats – A review [J]. Renewable and Sustainable Energy Reviews, 2024, 189(PA):

[3] Cruz, C. N, Redondo, et al. Optimizing the Heliostat Field Layout by Applying Stochastic Population-Based Algorithms [J]. Informatica, 2018, 29(1): 21-39.

[4] Qiyue X, Ziqi G, Daifei L, et al. Optimization of heliostat field distribution based on improved Gray Wolf optimization algorithm [J]. Renewable Energy, 2021, 176447-458.

[5] A. A R, Dong Y. A detailed account of calculation of shading and blocking factor of a heliostat field [J]. Renewable Energy, 2022, 181292-303.

[6] Yang S, Lee K, Lee I. Pattern-free heliostat field layout optimization using physics-based gradient [J]. Solar Energy, 2020, 206722-731.

[7] Wen-Qi W, Rui J, Ya-Ling H, et al. Optical-thermal-mechanical analysis of high-temperature receiver integrated with gradually sparse biomimetic heliostat field layouts for the next-generation solar power tower [J]. Solar Energy, 2022, 23235-51.

[8] Muhammad H, Ur A R, Sheeraz I, et al. Genetic algorithm optimization of heliostat field layout for the design of a central receiver solar thermal power plant [J]. Heliyon, 2023, 9(11): e21488-e21488.

[9] A.A R, N.S D, Abdelrahman E, et al. A review and classification of layouts and optimization techniques used in design of heliostat fields in solar central receiver systems [J]. Solar Energy, 2021, 218296-311.

[10] Yang S, Lee K, Lee I. Pattern-free heliostat field layout optimization using physics-based gradient [J]. Solar Energy, 2020, 206722-731.